Published by Avanti Publishers

Journal of Advanced Thermal Science Research

ISSN (online): 2409-5826

Research on the Thermal Runaway Characteristics and Evolution of NCA Lithium-ion Cells under Transportation Vibration and High Temperature

Songli Zhang[1], Zhenyan Liu[1] and Yanli Zhu[1,2,*]

[1]State Key Laboratory of Explosion Science and Technology, Beijing Institute of Technology, Beijing 100081, China
[2]Chongqing Innovation Center, Beijing Institute of Technology, Chongqing 401120, China

ARTICLE INFO

Article Type: Research Article

Academic Editor: Weiguang Su

Keywords:
Vibration
High temperature
Thermal runaway
Lithium-ion battery
Thermal runaway mechanism

Timeline:
Received: August 31, 2025
Accepted: October 15, 2025
Published: November 18, 2025

Citation: Zhang S, Liu Z, Zhu Y. Research on the thermal runaway characteristics and evolution of NCA lithium-ion cells under transportation vibration and high temperature. J Adv Therm Sci Res. 2025; 12: 38-52.

DOI: https://doi.org/10.15377/2409-5826.2025.12.3

ABSTRACT

This paper investigates the effects of vibration and high temperature, two typical transportation conditions, on the thermal runaway characteristics of 18650 NCA cells through simulation experiments. The aim is to explore the mechanisms by which transportation conditions affect the thermal runaway behavior and safety degradation of lithium-ion cells. The results show that both vibration and high temperature lead to slight capacity decay (a decrease of 0.49% and 0.38% respectively) and a significant increase in internal resistance (an increase of 24.59% and 20.49% respectively), thereby increasing the risk of thermal runaway. The thermal runaway venting temperature of NCA cells subjected to vibration and high temperature is raised by 12.04°C and 6.08°C respectively, with the venting time occurring earlier. The thermal stability of the cells is reduced, while the thermal runaway temperature is significantly lowered, with the vibration and high temperature samples decreasing by 40.85°C and 31.28°C respectively. The critical time is also shortened by 232s and 211s respectively, indicating that the overall thermal runaway process is significantly accelerated. Material analysis reveals that vibration causes structural fractures, while high temperature promotes side reactions in advance, both of which lead to accelerated thermal runaway reactions and intensified heat release. This is macroscopically manifested as a decrease in thermal runaway temperature and an increase in the highest temperature.

*Corresponding Author
Email: zhuyanli1999@bit.edu.cn
Tel: +(86) 18601097870

1. Introduction

1.1. Background

Lithium-ion batteries, due to their excellent high energy density, long cycle life, and environmentally friendly characteristics, have demonstrated broad application prospects in the field of electric energy storage and have become the preferred medium in the energy storage and supply field, widely used in the power supply fields of new energy vehicles and electronic products [1-4]. The global market demand for lithium-ion batteries continues to grow rapidly, significantly driving the rapid expansion of the industry worldwide. China, as the world's largest producer and consumer market for power lithium batteries, has a particularly prominent scale of product transportation. The rapid growth in global demand for lithium-ion batteries continues to drive the rapid expansion of the industry worldwide, especially in China. Statistics show that the annual transportation volume of power lithium batteries in China has exceeded one hundred billion kilowatt-hours, including both domestic and exported lithium battery products [5-6]. Among them, the inter-provincial transportation of batteries for new energy vehicles accounts for the main part and shows an increasing trend year by year. With the increasingly widespread application of lithium-ion batteries, concerns about battery safety are on the rise [7]. The transportation process is a continuous one that can affect its performance [8, 9].

However, during long-distance or complex condition transportation, batteries inevitably experience severe environmental conditions such as continuous vibration and temperature changes [10, 11]. These external factors may affect the safety, electrochemical performance, and service life of batteries. For instance, extreme temperatures can significantly impact the performance and lifespan of lithium-ion batteries, potentially leading to safety issues such as fires. Accidents during transportation occur from time to time [12, 13], and these external factors may affect the safety, electrochemical performance, and service life of batteries, which have become the focus of attention in both academic and industrial fields.

1.2. Research on Safety of Lithium-Ion Batteries Under Transportation Conditions

Batteries often undergo prolonged vibration during transportation, which may have an irreversible impact on their safety. Vibration refers to the mechanical oscillation in a system caused by dynamic forces, mechanical stress or external excitation. In engineering systems, vibration may be caused by operating machinery, external environmental factors, or inherent material behavior [14,15]. Zhang *et al*. [16] conducted vibration durability tests on NCA lithium-ion 18650 battery cells and studied the influence of vibration on the electrical performance of lithium-ion batteries based on mathematical statistical analysis. Vibration may cause minor changes in the internal structure of the battery, thereby affecting its electrochemical properties. At the same time, vibration will accelerate the aging process of the battery and reduce its service life. Hooper *et al*. [17] conducted vibration durability tests on nickel-manganese-cobalt oxide (NMC) lithium-ion 18650 battery cells and also found that vibration has a negative impact on battery performance. In his other study [18], the vibration input of high-voltage batteries in electric vehicles was characterized. Research has found that the vibration frequency and intensity generated during vehicle operation have a significant impact on the performance and safety of 18650 lithium batteries. Yuk *et al*. [19] investigated the safety of 18650 lithium-ion batteries under different vibration conditions. Research indicates that vibration may cause short circuits or thermal runaway inside batteries, thereby leading to safety issues. Existing research indicates that vibration conditions can cause structural damage inside batteries, thereby accelerating battery aging, affecting electrical performance, reducing safety, and increasing the risk of thermal runaway. Brand *et al*. [20] demonstrated that vibration loads might cause unique internal damage that is typically uncommon in standardized tests. Research has found that prolonged vibration stress can cause internal structural failures in lithium-ion batteries, such as short circuits and material displacement, with cylindrical batteries being particularly at risk. He *et al*. developed an adaptive fuzzy reasoning model to evaluate the durability of lead-acid batteries under vibration, thereby enabling accurate real-time detection without causing severe damage. This highly adaptable method offers potential for evaluating lithium-ion batteries, especially when electric vehicles are exposed to more complex mechanical environments [21]. In the automotive field, the pre-consistency vibration test of lithium iron phosphate battery packs ensures long-term reliability by simulating real-world dynamic loads, thereby helping to maintain structural stability during the use of electric powertrains [22]. Research has found that internal damage to 18650 lithium-ion batteries, especially in the loosely designed mandrel, does not immediately

reduce performance under vibration. Researchers used computed tomography (CT) scans to visualize subtle structural faults that became severe over time, highlighting the necessity of robust internal cell design [23]. Bangal *et al*. used electrochemical impedance spectroscopy (EIS) to track the changes in the internal resistance of batteries under vibration force, which is particularly useful in the health diagnosis of electric vehicle batteries [24].

During transportation, extreme high-temperature weather is often encountered. Lithium-ion batteries are kept in closed packaging for a long time. Existing research indicates that storing lithium-ion batteries at high temperatures can significantly affect battery performance, including capacity degradation, increased internal resistance, damage to the solid electrolyte interface (SEI) film, and electrolyte consumption [25-28]. Lang *et al*. [29] investigated the influence of storage temperature on the aging mechanism of calendars and found that the capacity loss mainly resulted from the loss of recyclable lithium ions due to side reactions on the anode surface, which accelerated sharply with the increase in temperature. Sarasketa-Zabala *et al*. [30] reported that as the storage temperature rises, capacity loss will be significantly accelerated. Nemati *et al*. [31] observed that at a storage temperature of 55°C, the surface material of the anode fell off, and the active substances were further lost. Due to the poor heat dissipation inside the closed space, heat accumulation is prone to occur. In a high-temperature environment, the internal chemical reactions of lithium-ion batteries accelerate, which will lead to an increase in the internal pressure of the battery, thereby affecting the battery's cycle life and safety. Feng *et al*. [32-34] analyzed the common behaviors of thermal runaway using an adiabatic accelerated calorimeter (ARC) and divided the process into three stages based on the critical point of thermal runaway. Zhang *et al*. [35] analyzed the high-temperature storage of NCM (631) pouch cells at 60 °C with 100% SOC. They found that a decrease in the TR characteristic temperature indicates an increased possibility of TR occurrence in the battery. Cai *et al*. [36] studied 18,650 NCM cells stored at short-term high temperatures of 60°C and 80°C. Based on the characteristic temperatures of battery thermal runaway, they indicated that the possibility of TR increased and its severity rose. Chombo *et al*. [37] used a 0.6kW heater to study the effect of heating on the performance of 18650 lithium-ion batteries. Research has found that high-temperature heating can lead to a significant decline in the electrochemical performance of batteries, including capacity attenuation and increased internal resistance. Moreover, high-temperature heating also accelerates the aging process of batteries and reduces their service life. Ubaldi *et al*. [38] identified key events and gas emissions during the thermal runaway process of NCA18650 batteries through thermal abuse tests. The experimental results show that during the thermal runaway process, the battery releases a large amount of heat and gases, including hydrofluoric acid (HF), carbon dioxide (CO_2), and carbon monoxide (CO). Jones [39] explored the impact of high-temperature storage on the performance of 18650 lithium batteries and found that high temperatures would accelerate the aging process of the battery, leading to capacity decline and increased internal resistance. Ren *et al*. [40] studied the disappearance of the exothermic peak of the negative electrode at around 300 °C after high-temperature storage, and believed that it was caused by the reduced lithiation degree of the negative electrode after aging. Zhang *et al*. [41] investigated the effects of two aging conditions, namely short-term high-temperature storage and post-storage recirculation, on the internal side reactions of NCM523 ternary lithium-ion batteries. Based on the DSC results, the authors mentioned that the heat generation of the reaction between the positive electrode and the electrolyte as well as the related side reactions of the negative electrode increased after aging, but neither was significant. Zhang *et al*. [42] investigated the effect of high-temperature calendar aging on the side reactions of NCM631 ternary batteries, indicating that the temperature for the SEI film decomposition reaction decreased. Research indicates that under high-temperature storage conditions, the self-discharge rate of batteries significantly increases, and the decomposition reaction of the electrolyte intensifies, reducing battery safety.

During transportation, vibration and high temperature are two key environmental factors that affect the safety and performance of lithium-ion batteries. Existing research indicates that continuous vibration can cause mechanical damage to the internal structure of batteries, leading to the shedding of electrode active materials, an increase in internal resistance, and accelerated aging, thereby increasing the risk of thermal runaway. Multiple vibration experiments on 18650 batteries based on NCA and NMC systems have confirmed that the complex vibration spectra in actual transportation conditions can significantly affect the electrochemical performance and safety of the batteries. On the other hand, high-temperature environments will intensify the side reactions inside the battery, promoting the decomposition of the electrolyte, gas production and an increase in internal pressure, resulting in capacity attenuation and a reduction in cycle life. Thermal abuse tests further indicate that high temperatures not only accelerate battery aging but also trigger the release of a large amount of heat and harmful

gases, significantly increasing the possibility of thermal runaway. However, most of the existing studies are based on laboratory conditions and have not simulated the vibration and high-temperature working conditions during transportation, thus failing to reflect the thermal runaway mechanism of batteries under transportation conditions. This type of research method has obvious limitations: The simple harmonic vibration mode adopted is significantly different from the random vibration spectrum actually encountered during transportation. Meanwhile, high-temperature experiments typically employ adiabatic accelerated calorimeters (ARC), under which the battery is in an adiabatic environment. Moreover, the experimental temperature is high and the duration is short, making it difficult to accurately predict the thermal safety performance of the battery in real transportation conditions.

1.3. Research Content

This study takes the 18650 lithium nickel cobalt aluminum oxide (NCA) cells with a state of charge (SOC) of 50% as the object and systematically investigates its safety under typical transportation conditions, including vibration and high-temperature environments. Immediately after the simulated transportation condition test, a thermal runaway test was conducted on the cells to analyze the influence of mechanical and thermal stress during transportation on the thermal runaway behavior of the cells. To further reveal its influence mechanism, the reaction was terminated by rapid cooling with liquid nitrogen at different stages of the thermal runaway process to retain the physicochemical state of the cells in this transient state. Microscopic characterization methods such as X-ray diffraction (XRD), scanning electron microscopy (SEM), and thermogravimetric - differential scanning calorimetry (TG-DSC) were employed. A systematic analysis was conducted on the structure, surface morphology and thermal stability evolution of electrode materials to clarify the intrinsic mechanism by which transportation conditions affect the thermal safety performance of lithium-ion cells. This study has for the first time established a full-chain research system covering transportation condition simulation, thermal safety testing, and microscopic mechanism analysis. Through multi-scale characterization, it has revealed the battery thermal runaway mechanism under the effects of vibration and high temperature during transportation, filling the gap in the research on the correlation between actual transportation conditions and battery safety performance.

2. Experimental Objects and Methods

2.1. Research Methods

The technical route of this research is shown in Fig. (**1**), mainly including three core parts. Firstly, for the 18650 NCA cells, experimental research was carried out to simulate extreme transportation environments. The vibration

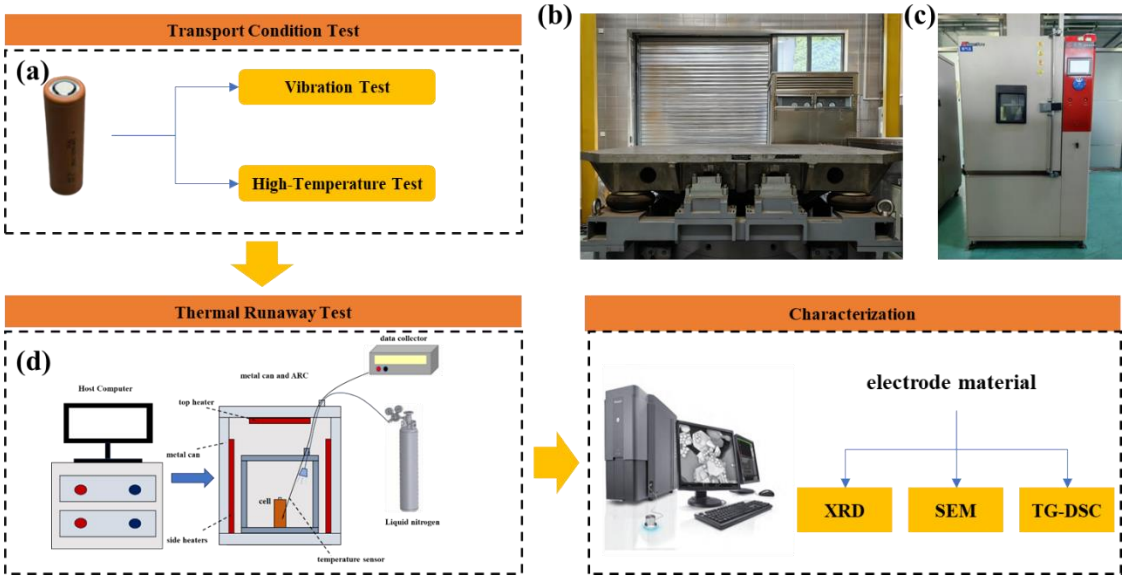

Figure 1: Experimental methods and platforms: (**a**) NCA cell; (**b**) vibration test bench; (**c**) high-temperature test chamber; (**d**) ARC test platform.

test was conducted in accordance with the ISTA 3E standard spectrum, and the high-temperature test was set under the storage condition of 85°C. By comparing the changes in cell capacity and internal resistance before and after the test, the influence of transportation conditions on cell electrical performance and its failure mechanism were analyzed. The second part focuses on the thermal safety of cells. Thermal runaway tests are conducted on cells treated under the above-mentioned transportation conditions using an adiabatic accelerated calorimeter (ARC), with a particular emphasis on the variation patterns of the critical temperature of thermal runaway and characteristic parameters. The third part focuses on the microscopic mechanism analysis at the material level. XRD, SEM and TG-DSC tests are carried out on cell samples after the termination of different thermal runaway stages. Through the characterization results of material structure, morphology and thermal stability, the key features in the evolution process of thermal runaway under the influence of transportation conditions are extracted, thereby revealing the internal mechanism that leads to the reduction of cell thermal safety. The overall research follows a systematic analysis path from macroscopic performance to microscopic mechanisms.

2.2. Transportation Condition Testing

In this experiment, 18650 lithium-ion cells with a nominal capacity of 3.5 Ah and a NCA system were used. The measured capacity at a 1C rate ranged from 3.4 to 3.6 Ah. The specific performance parameters are shown in Table **1**. The state of charge (SOC) of cell is usually controlled below 50%. Thermal runaway (TR) of lithium-ion batteries is related to their SOC, and an increased risk of TR has been observed at higher SOC levels [43-47]. For safety purposes, batteries are usually kept at a low SOC [48]. Therefore, in this study, 50% SOC is selected as the typical working condition. In the setting of transportation environment parameters, the vibration spectrum adopts the ISTA 3E standard [49], and the selected frequency band is 1-200Hz. This spectrum is constructed based on the vibration data collected in actual road transportation to simulate global transportation severely and realistically, especially the complex random vibration stress encountered in road transportation. The high-temperature conditions refer to the research of Guddanti *et al*. [50]. The extreme transportation temperature is set at 85°C, and the test time parameters are all 12 hours. The specific experimental parameters are shown in Table **2**.

Table 1: Specifications of the LIB.

Terms	Rating
Cathode material	NCA
Anode material	Graphite
Nominal capacity/ Ah	3.55Ah
Nominal voltage/V	3.6V
cut-off voltage/V	4.2V/2.5V
Size/mm	65.3mm×18.55mm
Weight/ g	46±5g

2.3. ARC Test

This experiment takes the NCA cells that has undergone vibration and high-temperature transportation condition tests in Section 2.2 as the research object. The nominal capacity of the cell is 3.5 Ah. The cell numbers used in the test and the corresponding treatment conditions are shown in Table **3**, where t_{OP} represents the opening time of the cells safety valve and t_{TR} represents the moment when the cell experiences thermal runaway.

The thermal runaway characteristics of lithium-ion cells were tested by using an Accelerating Rate calorimeter (ARC), and the layout of the experimental platform is shown in Fig. (**1d**). The temperature rise behavior, key temperature characteristics and thermal runaway evolution law of the cell under thermal abuse conditions can be obtained through the ARC experiment. The specific experimental steps are as follows:

Table 2: Vibration test spectrum.

Frequency (Hz)	PSD(g^2/Hz)
1.0	0.00072
3.0	0.018
4.0	0.018
6.0	0.00072
12.0	0.00072
16.0	0.0036
25.0	0.0036
30.0	0.00072
40.0	0.0036
80.0	0.0036
100.0	0.0036
200.0	0.000018

Table 3: Test LIBs identification numbers.

Test Condition	Untested	Vibration	High-Temperature
Unheated	U-t_0	V-t_0	H-t_0
Vent Opening	U-t_{OP}	V-t_{OP}	H-t_{OP}
Thermal Runaway onset	U-t_{TR}	V-t_{TR}	H-t_{TR}
Post-Thermal Runaway	U-t_1	V-t_1	H-t_1

1) Place the cell to be tested in the ARC sample cell and fix the armored K-type thermocouple at the center of the cell surface with high-temperature resistant tape to ensure the accurate collection of temperature signals

2) The ARC is set to perform constant temperature heating at 200°C through the upper computer control program. The surface temperature changes of the cell are monitored and recorded in real time. Once the system determines that the cell has entered a thermal runaway state, the heating is immediately stopped.

3) Implement differentiated cooling and sampling procedures for cells of different numbers: For the numbered t_{OP} cells, immediately turn off the heater after the safety valve is opened, and inject liquid nitrogen into the reaction chamber for rapid cooling to freeze the material reaction in this state. For the numbered t_{TR} cells, heating is stopped at the moment of thermal runaway and liquid nitrogen is also introduced for rapid cooling to preserve the material characteristics of the initial stage of thermal runaway. The above two groups of cells were disassembled in the glove box to obtain the positive and negative electrode active materials respectively, which were used for subsequent microstructure characterization. The cells numbered t_0 was used as the control group and was directly disassembled without heating treatment to provide the reference sample in its original state. Cells No. t_1 is not cooled after thermal runaway occurs and is allowed to cool naturally to record the complete temperature curve for analyzing the critical temperature of thermal runaway and the maximum temperature T_{max}.

2.4. Characterization of Electrode Materials

For the cells of sequence t_{OP} and t_{TR}, after being heated to the corresponding characteristic points respectively by a unified heating method, they are immediately rapidly cooled by liquid nitrogen to terminate the reaction.

After the cells have returned to room temperature, it is disassembled in an argon-protected glove box, and the positive and negative electrode sheets are taken out respectively as test samples. Subsequently, the crystal structure, surface morphology and thermal stability of the electrode materials were characterized by X-ray diffraction (XRD), scanning electron microscopy (SEM) and thermogravimetric - differential scanning calorimetry (TG-DSC). XRD testing was conducted using a benchtop X-ray powder diffractometer (model: BRUKER D2 PHASER) produced by Bruker, a German company, to analyze the phase structure of materials. SEM observation was conducted using the Phenom ProX G6 scanning electron microscope from Phenom of the Netherlands. Microscopic morphology images of electrode materials were obtained under the conditions of an acceleration voltage of 15 kV and a uniform magnification of 5000 times. The thermal stability test was accomplished by connecting a synchronous thermal analyzer (model: NETZSCH STA449C) from Netzsch, Germany, to a mass spectrometer (NetzSCH-QMS403C). During the test, approximately 3 mg of the sample was placed in an alumina crucible and heated at a rate of 10°C ·min^{-1} from 30°C to 600°C under the protection of a 50 mL·min^{-1} high-purity argon atmosphere. The mass of the material and the changes in heat flow were recorded in real time.

3. Results and Discussion

3.1. Electrical Performance Test

After the cell underwent transportation condition tests, the changes in cell capacity and internal resistance are shown in Fig. (**2**). For each test, three cells with similar capacities were selected for parallel tests (vibration test cells: V1,V2,V3; high-temperature test cells: H1,H2,H3). The values in the table are the average values taken after the three tests. The error bars and statistical significance analysis demonstrate that the battery performance degradation and thermal safety changes induced by the transportation conditions, as reported in this paper, represent statistically significant and reliable conclusions. The results show that both vibration and high-temperature conditions lead to a slight decline in cell capacity (by 0.49% and 0.38% respectively). The internal resistance of the cell has significantly increased, with vibration causing an average increase of 24.59% in the cell's internal resistance. High temperatures increase the average internal resistance of cell by 20.49%. The increase in internal resistance will raise the Joule heat generated during short circuits within the cell, significantly increasing the risk of thermal runaway.

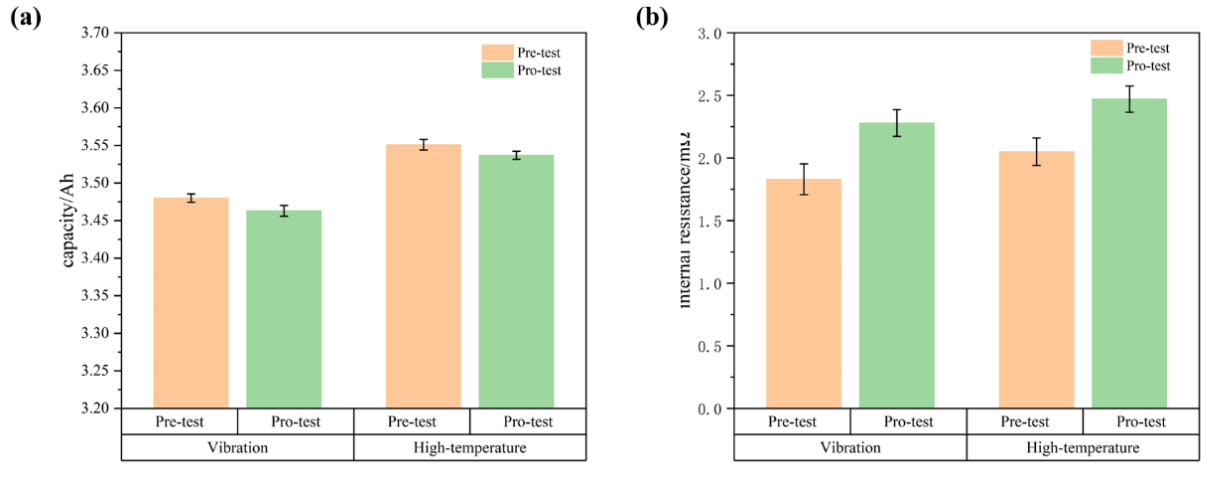

Figure 2: Changes in cell parameters before and after testing: (**a**) capacity; (**b**) internal resistance.

3.2. Critical Parameters of Thermal Runaway

To clarify the influence of two typical transportation conditions, vibration and high temperature, on the thermal safety behavior of lithium-ion cells, this study conducted thermal runaway experiments on cells samples after different pretreatments and compared and analyzed the temperature evolution curves at time t_1 (i.e., when the cell undergoes a complete thermal runaway process). To clarify the influence of two typical transportation

conditions, vibration and high temperature, on the thermal safety behavior of lithium-ion cells, this study conducted thermal runaway experiments on cell samples after different pretreatments and compared and analyzed the temperature evolution curves at time t_1 (i.e., when the cells undergoes a complete thermal runaway process).

The thermal runaway valve breaking temperatures of NCA cells after vibration and high temperature increased by 12.04°C and 6.08°C respectively, but the valve breaking times were shortened by 332s and 306s respectively. This indicates that the thermal stability of cells under transportation conditions decreases, self-heat generation occurs earlier, and the heat generation is greater. The thermal runaway temperature was significantly reduced. The vibration and high-temperature samples decreased by 40.85°C and 31.28°C respectively, indicating that the transportation conditions exacerbated the side reactions or structural damage of the internal materials of the cell, causing thermal runaway to occur at a relatively low temperature. Meanwhile, the thermal runaway time was shortened by 232 seconds and 216 seconds respectively, suggesting that the evolution process of cell thermal runaway has accelerated. It is particularly worth noting that the maximum temperature of the cell under high-temperature conditions reached 606.25°C, which was 91.82°C higher than that of the new cells and 70.90°C higher than that of the vibration sample. This indicates that the high-temperature transportation environment significantly intensified the intensity of the cells reaction. Meanwhile, the critical times were shortened by 232 seconds and 211 seconds respectively, and the overall process of thermal runaway was significantly accelerated (Table **4**).

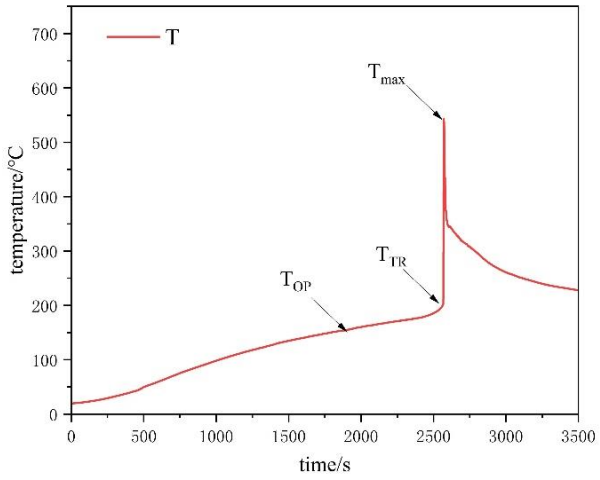

Figure 3: Critical temperature for cell thermal runaway.

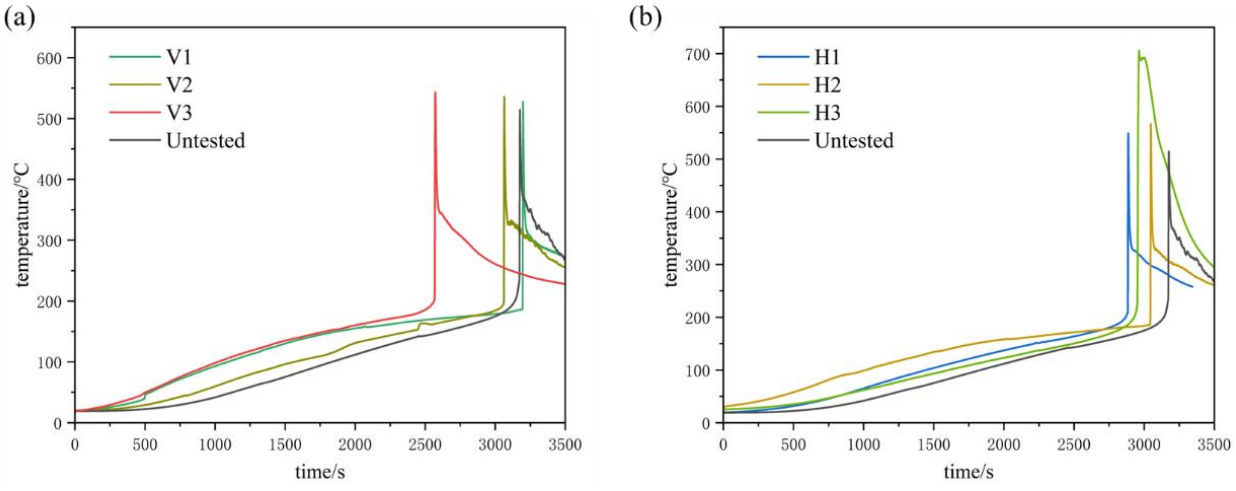

Figure 4: Cells thermal runaway temperature curve.

Table 4: Test LIBs identification numbers.

Temperature/℃	Untested	Vibration Tested	High-Temperature Tested
T_{OP}	142.96	155.00	149.04
T_{TR}	235.85	195.00	204.57
T_{max}	514.43	535.35	606.25
t_{OP}	2475	2143	2169
t_{TR}	3172	2940	2956
t_{max}	3176	2944	2965

3.3. Material Characterization Material Characterization

Fig. (**5**) shows the changes in XRD diffraction patterns of the positive and negative electrode materials of NCA cells treated under different transportation conditions at different stages of thermal runaway. Before heating, the cathode materials of all cells presented typical $LiNiCoAlO_2$ layered structure characteristic peaks (marked as A, B, and D peaks), while the anode was mainly composed of lithium-intercalated graphite, mainly showing characteristic diffraction peaks of LiC_{12} and LiC_6.

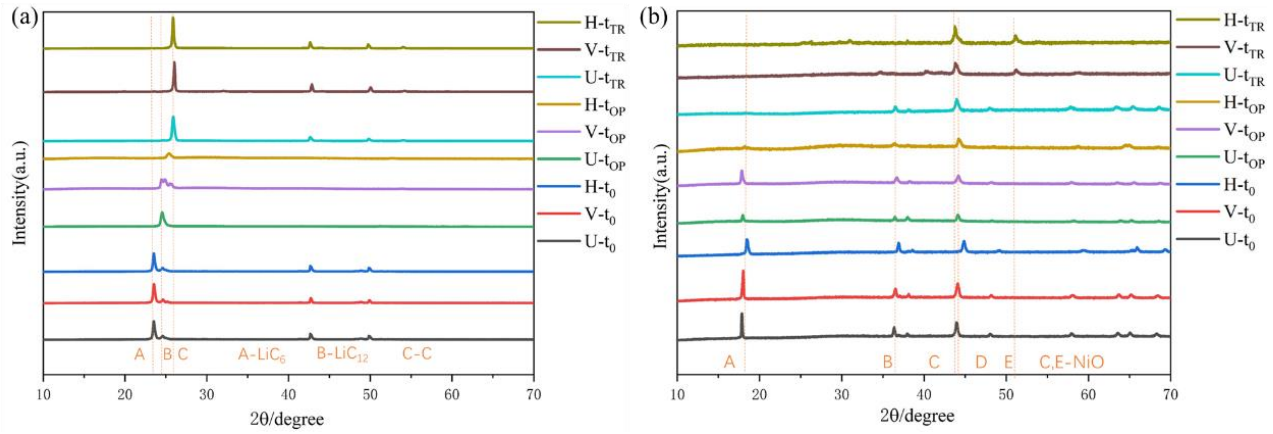

Figure 5: XRD patterns of cell materials at different stages of thermal runaway: (**a**) Negative electrode; (**b**) Positive electrode.

By the time the safety valve opens (t_{OP}), the diffraction peaks of the negative electrode material undergo a significant transformation: the intensity of the characteristic peaks of LiC_6 and LiC_{12} weakens and gradually evolves towards the characteristic peaks of the (002) crystal plane of graphite, indicating that the lithium-intercalating compounds of the negative electrode undergo a delithiation reaction, and the active lithium is continuously consumed due to its participation in interfacial side reactions ($LiC_6 \rightarrow LiC_{12} \rightarrow C$). During this transformation process, the reaction degree of the cells treated under high-temperature conditions was the most significant, with its characteristic peak approaching that of pure graphite earliest, while the change range of the new cells was the smallest, indicating that the high-temperature environment exacerbated the loss of active lithium. Meanwhile, there are also signs of structural evolution in the cathode material: the characteristic peak of $LiNiCoAlO_2$ has shifted, among which the intensity of peak A, which represents the crystal plane of the layered structure (003), has decreased or even gradually disappeared, while the position of peak D has shifted significantly, especially in high-temperature storage cells, indicating that the cathode material has undergone phase transformation and degradation of the layered structure. At the moment of thermal runaway (t_{TR}), the characteristic diffraction peaks of the cathode material completely disappear and transform into broad diffuse peaks such as NiO without lithium oxides, indicating the complete collapse of the layered structure, accompanied by the reduction of nickel elements and the formation of oxides. At this point, there is no diffraction signal of lithium compounds at the negative electrode. Only the standard diffraction characteristics of graphite crystals are

displayed, indicating that the active lithium has been completely consumed, while the main structure of the graphite is still retained. The above results indicate that as the thermal runaway process advances, the active materials of the positive and negative electrodes undergo continuous decay and phase transformation, and the high-temperature transportation conditions significantly accelerate this degradation process.

Fig. (**6**) and (**7**) respectively show the SEM images of the negative and positive electrode materials of NCA cells under different working conditions and at different stages of thermal runaway. Before heating, from the perspective of the negative electrode, the active material of the cell that had not undergone the transportation condition test was evenly distributed. However, after the vibration test, obvious cracks were observed on the cell surface, which was very likely due to the shedding and fragmentation of the active material caused by the vibration condition. On the other hand, after the high-temperature test, some deposits appeared on the cell surface, which might be caused by the decomposition of the SEI film. From the perspective of the positive electrode, the positive electrode material that has not undergone the transportation condition test is evenly distributed. After the vibration test, some cracks were observed on the cell surface, which has similar characteristics to the negative electrode material. However, the positive electrode material that has undergone the high-temperature test shows local defects, which looks like the shedding of some materials. At the moment of gas generation, the adherents on the surface of the blocky graphite at the negative electrode disappear, and the outline becomes clearer. The blocky graphite gradually shatters into smaller particles. Among them, after high-temperature storage, the negative electrode material of the cell gradually becomes powderized, and many deposits also appear on the surface. There is a relatively obvious powdering phenomenon in the cathode material, with the material particles becoming smaller. The surface particles of the vibrating cell fall off, cracks expand, and large particles in the deep interior are exposed. Many small particle deposits appear on the surface of the high-temperature cell, which may be the side reaction products between the cathode material and the electrolyte. At the moment of thermal runaway, the negative electrode material is almost completely damaged, and the chemical reaction products caused by side reactions lead to a significant increase in particle deposits. The gap between the particles of the positive electrode material increases, and the intense reaction causes the material to completely shatter.

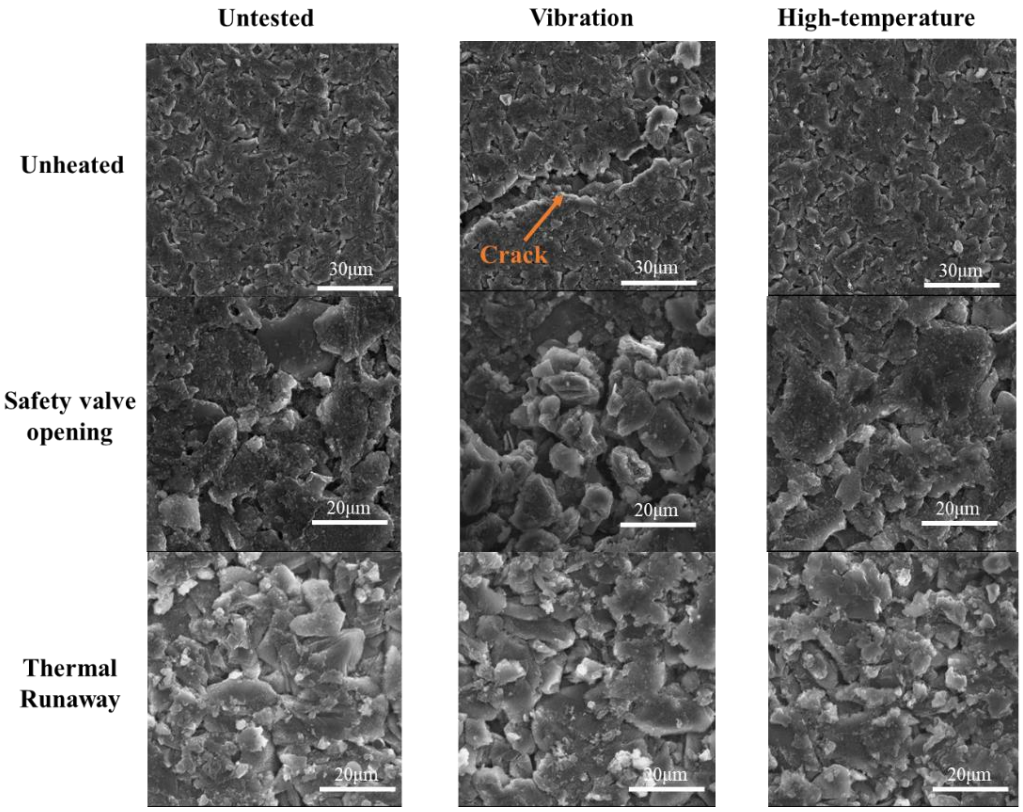

Figure 6: SEM image of the negative electrode of the cells.

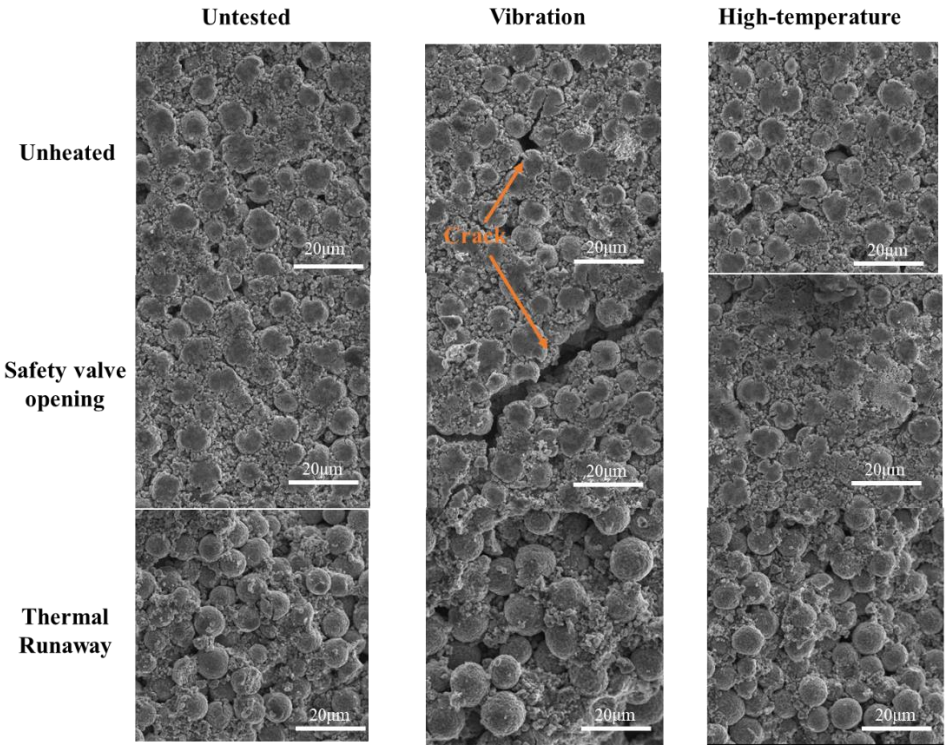

Figure 7: SEM image of the positive electrode of cells.

Fig. (**8**) shows the TG-DSC analysis results of the cathode materials of NCA cells treated under different transportation conditions at each stage of thermal runaway. Similar to NCM materials, the thermal decomposition process of NCA cathode materials can be divided into three distinct weight loss stages according to its TG curve, with the two characteristic inflection point temperatures located around 150°C and 468°C respectively.

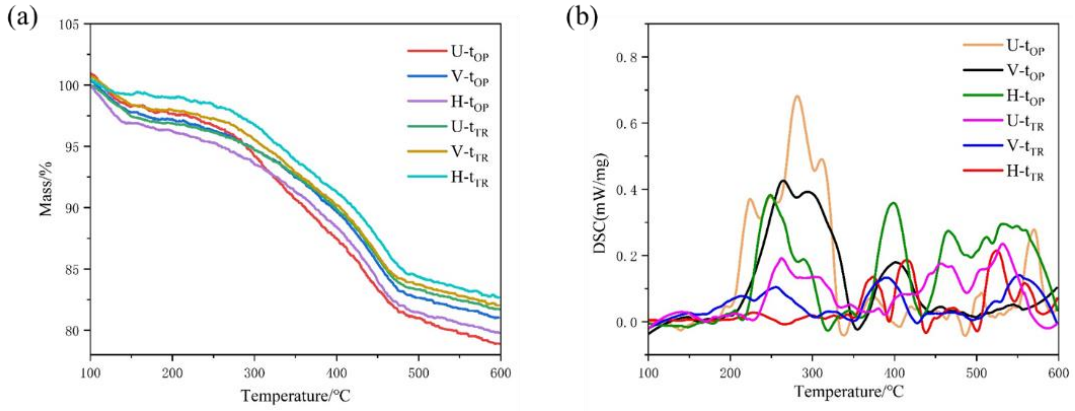

Figure 8: TG-DSC diagrams of cathode materials at different thermal runaway stages: (**a**) TG; (**b**) DSC.

The first stage (room temperature to 150°C) mainly corresponds to the evaporation of organic solvents adsorbed or remaining on the surface of the cathode material, as well as the melting and initial decomposition of the separator (such as PE/PP). This stage is manifested on the DSC curve as a series of complex endothermic and exothermic peaks, reflecting the competition among various physical phase transitions and chemical decomposition reactions. The second stage (150°C to 468°C) is mainly characterized by the decomposition reaction of lithium-containing cathode active substances (such as $LixNiCoAlO_2$). As lithium ions are released (x decreases), the stability of the layered structure decreases, the decomposition reaction intensifies, and the exothermic peak in the DSC curve gradually shifts towards higher temperatures, indicating an increase in the activation energy required for the reaction. It is worth noting that the new cell (which has not undergone

transportation conditions) has the lowest exothermic peak temperature and the highest peak intensity at this stage, indicating that its active lithium content is relatively high and the rate of side reactions is relatively slow. Cells that have undergone vibration or high-temperature pretreatment exhibit characteristics of forward reaction and right shift of exothermic peaks, reflecting the loss of active lithium and damage to the material structure. The third stage (above 468°C) mainly involves the further oxidation of transition metal elements (Ni, Co, Al) in the cathode and the formation of oxides, accompanied by a significant exothermic effect. The DSC curve of the thermal runaway cell shows sharp and concentrated exothermic peaks in this range, indicating that this stage is a key period for the concentrated release of energy during the thermal runaway process.

3.4. Mechanism Summary

Based on the segmented thermal runaway experiments and the microscopic characterization analysis of materials, combined with the performance degradation and failure behavior of the cell after the transportation condition test and the changes in the critical parameters of thermal runaway, the mechanism of thermal runaway of power cells under transportation conditions can be summarized as follows:

(1) The influence mechanism of vibration conditions: Mechanical vibration causes fatigue, shedding and even fracture of the active materials of the electrodes inside the cell (positive and negative electrodes), resulting in reversible loss of lithium ions, leading to a significant increase in cell capacity and internal resistance. The increase in internal resistance causes the cell to generate more Joule heat when an internal short circuit occurs, significantly raising the risk of thermal runaway triggering. Meanwhile, the material fragmentation caused by vibration increases the contact area between the electrode and the electrolyte, accelerating the kinetic process of interfacial side reactions. In addition, vibration may also cause uneven distribution of the electrolyte, leading to local heat dissipation differences in the cell under thermal abuse conditions, which is prone to form high-temperature hotspots. This, on a macroscopic level, is manifested as a decrease in the thermal runaway trigger temperature (T_{TR}) and an increase in the intensity of the reaction.

(2) The influence mechanism of high-temperature working conditions: The high-temperature environment intensifies the side reactions at the electrode/electrolyte interface, especially causing irreversible decomposition and reconstruction of the SEI film on the negative electrode surface, continuously consuming active lithium, and promoting the premature decomposition and gas production of some low-melting-point and low-flash point electrolyte components. These processes cause the cells cell capacity to decline and the internal resistance to increase, and the negative electrode active material to lose the protection of the SEI film and be directly exposed to the electrolyte, thereby significantly accelerating the chain exothermic reaction in the thermal runaway stage. The above-mentioned microscopic-level changes are directly reflected in the macroscopic thermal behavior as a decrease in the thermal runaway trigger temperature (T_{TR}), a significant increase in the maximum temperature (T_{mmm}), and a sharp shortening of the entire thermal runaway process.

4. Conclusion

This study systematically evaluates the performance evolution and thermal safety mechanisms of 18650 NCA lithium-ion batteries under vibration and high-temperature transportation conditions. The main conclusions are as follows:

(1) Transportation conditions accelerate the degradation of battery electrical performance. Both vibration and high-temperature environments lead to capacity fade (0.49% for vibration group, 0.38% for high-temperature group) and significant increase in internal resistance (24.59% for vibration group, 20.49% for high-temperature group). The increased internal resistance exacerbates Joule heating during short circuits, elevating thermal runaway risk. Microscopic characterization reveals that vibration causes detachment of electrode active materials, while high temperature intensifies side reactions at the electrode-electrolyte interface, resulting in active lithium loss.

(2) Vibration conditions significantly reduce battery thermal stability. After vibration testing, the venting temperature increases by 12.04°C, venting time advances by 332 seconds, thermal runaway temperature

decreases by 40.85°C, and the thermal runaway evolution process accelerates by 232 seconds. Material analysis indicates that vibration induces electrode material fracture, increasing the electrode-electrolyte contact area while causing uneven electrolyte distribution that creates local hot spots. These factors accelerate reaction kinetics, promoting thermal runaway at lower temperatures.

(3) High-temperature conditions intensify battery reaction severity. After high-temperature testing, the maximum battery temperature reaches 606.25°C, representing increases of 91.82°C and 70.90°C compared to fresh batteries and vibrated samples, respectively. The critical times for thermal runaway are significantly shortened. Microscopic investigation demonstrates that high temperature promotes premature decomposition of the SEI film on the anode surface, eliminating its protective function and enhancing direct reactions between the anode and electrolyte. This accelerates the thermal runaway process and increases heat release intensity.

This research reveals the underlying mechanisms through which transportation conditions affect battery thermal safety via multi-scale experiments, providing a theoretical basis for establishing safety standards for power battery transportation.

Based on experimental data and mechanism analysis, this study proposes the following transportation safety suggestions: 1) State of charge control: It is recommended that the state of charge of power batteries during transportation be controlled within the range of 30% to 50%; 2) Packaging protection requirements: In view of the random vibration characteristics of road transportation, it is recommended to use composite cushioning materials with an elastic modulus of $\geq$5MPa, and design multi-layer irregular structures to attenuate the vibration energy in the 1-200Hz frequency band. 3) Transportation environment monitoring: Establish a full-process temperature control system. When the ambient temperature exceeds 65°C for 2 consecutive hours, the emergency heat dissipation mechanism should be activated, and vibration sensors should be installed inside the packaging to monitor the peak acceleration in real time.

Conflict of Interest

The authors declared that they have no conflicts of interest to this work. We declare that we do not have any commercial or associative interest that represents a conflict of interest in connection with the work submitted

Funding

This work is supported by National Key Research and Development Program of China (Grant No. 2023YFC3009501), the National Natural Science Foundation of China (Grant No. 52374298), and Beijing Natural Science Foundation (Grant No. L243019).

Acknowledgments

The authors gratefully acknowledge the financial support provided by the respective funding agencies mentioned above.

References

[1] Rengaswamy Srinivasan M, Thomas ME, Airola MB, Carkhuff BG, Frizzell-Makowski LJ, Alkandry H, *et al*. Preventing cell-to-cell propagation of thermal runaway in lithium-ion batteries. J Electrochem Soc. 2020; 167(2): 020559. https://doi.org/10.1149/1945-7111/ab6ff0

[2] Wang Q, Mao B, Stoliarov SI, Sun J. A review of lithium ion battery failure mechanisms and fire prevention strategies. Prog Energy Combust Sci. 2019; 73: 95-131. https://doi.org/10.1016/j.pecs.2019.03.002

[3] Zhang J, Zhang L, Sun F, Wang Z. An overview on thermal safety issues of lithium-ion batteries for electric vehicle application. IEEE Access. 2018; 6: 23848-63. https://doi.org/10.1109/ACCESS.2018.2824838

[4] Feng X, Lu L, Ouyang M, Li J, He X. A 3D thermal runaway propagation model for a large format lithium ion battery module. Energy. 2016; 115: 194-208. https://doi.org/10.1016/j.energy.2016.08.094

[5] Tabelin CB, Dallas J, Casanova S, Pelech T, Bournival G, Saydam S, *et al*. Towards a low-carbon society: A review of lithium resource availability, challenges and innovations in mining, extraction and recycling, and future perspectives. Miner Eng. 2021; 163: 106743. https://doi.org/10.1016/j.mineng.2020.106743

[6] Zheng L, Chen G, Liu L, Hu Y. Tracing of lithium supply and demand bottleneck in China's new energy vehicle industry—Based on the chart of lithium flow. Front Energy Res. 2022; 10: 992617. https://doi.org/10.3389/fenrg.2022.992617

[7] Li J, Zhang J, Zhang XG, Yang CZ, Xu NX, Xia BJ. Study of the storage performance of a Li-ion cell at elevated temperature. Electrochim Acta. 2010; 55(3): 927-34. https://doi.org/10.1016/j.electacta.2009.09.077

[8] Zulke A, Li Y, Keil P, Burrell R, Belaisch S, Nagarathinam M, *et al*. High-energy nickel-cobalt-aluminium oxide (NCA) cells on idle: anode- versus cathode-driven side reactions. Batteries Supercaps. 2021; 4(6): 934-47. https://doi.org/10.1002/batt.202100046

[9] Zhang Q, Wang DF, Schaltz E, Stroe DI, Gismero A, Yang BW. Lithium-ion battery calendar aging mechanism analysis and impedance-based state-of-health estimation method. J Energy Storage. 2023; 64: 107029. https://doi.org/10.1016/j.est.2023.107029

[10] Hua X, Thomas A. Effect of dynamic loads and vibrations on lithium-ion batteries. J Low Freq Noise Vib Act Control. 2021; 40(4): 1927-34. https://doi.org/10.1177/14613484211008112

[11] Zhang G, Wei X, Chen S, Wei G, Zhu J, Wang X, *et al*. Research on the impact of high-temperature aging on the thermal safety of lithium-ion batteries. J Energy Chem. 2023; 87: 378-89. https://doi.org/10.1016/j.jechem.2023.08.040

[12] Gao L, Chen M, Zhu J. Cause analysis of lithium battery air transportation accidents from the perspective of complex network analysis. In: International Conference on SmartRail, Traffic and Transportation Engineering. Singapore: Springer Nature Singapore; 2024. p. 352-9. https://doi.org/10.1007/978-981-96-7441-1_35

[13] Pan Y, Liu X, Wu J, Zhou H, Zhu L. Assessing lithium-ion battery safety under extreme transport conditions: a comparative study of measured and standardised parameters. Energies. 2025; 18(15): 4144. https://doi.org/10.3390/en18154144

[14] Hu G, Huang P, Bai Z, Wang Q, Qi K. Comprehensive analysis of failure evolution and safety evaluation of automotive lithium ion battery. eTransportation. 2021; 10: 100140. https://doi.org/10.1016/j.etran.2021.100140

[15] Esmaeili MH, Haft-Cheshmeh YM. Dynamic characteristics of elastomeric materials used as railway vibration mitigation measures considering the effect of shape factor. Measurement. 2024; 236: 115058. https://doi.org/10.1016/j.measurement.2024.115058

[16] Zhang L, Ning Z, Peng H, Mu Z, Sun C. Effects of vibration on the electrical performance of lithium-ion cells based on mathematical statistics. Appl Sci. 2017; 7(8): 802. https://doi.org/10.3390/app7080802

[17] Hooper JM, Marco J, Chouchelamane GH, Lyness C. Vibration durability testing of nickel manganese cobalt oxide (NMC) lithium-ion 18650 battery cells. Energies. 2016; 9(1): 52. https://doi.org/10.3390/en9010052

[18] Hooper JM, Marco J. Defining a representative vibration durability test for electric vehicle (EV) rechargeable energy storage systems (RESS). World Electr Veh J. 2016; 8(2): 327-38. https://doi.org/10.3390/wevj8020327

[19] Yuk S, Choi K, Park SG, Lee S. A study on the reliability test of a lithium battery in medical electric wheelchairs for vulnerable drivers. Appl Sci. 2019; 9(11): 2299. https://doi.org/10.3390/app9112299

[20] Brand MJ, Schuster SF, Bach T, Fleder E, Stelz M, Gläser S, *et al*. Effects of vibrations and shocks on lithium-ion cells. J Power Sources. 2015; 288: 62-9. https://doi.org/10.1016/j.jpowsour.2015.04.107

[21] He B, Wang H, He X. Vibration test methods and their experimental research on the performance of the lead-acid battery. J Power Sources. 2014; 268: 326-30. https://doi.org/10.1016/j.jpowsour.2014.05.098

[22] Eidinejad H, Madaro F, Brugo TM, Rossi C, Rivola A, Troncossi M, *et al*. Pre-compliance vibration testing of a LFP battery pack prototype for electric powertrains. In: 2024 IEEE International Workshop on Metrology for Automotive (MetroAutomotive); 2024 Jun 26-28; Bologna, Italy. https://doi.org/10.1109/MetroAutomotive61329.2024.10615669

[23] Berg P, Spielbauer M, Tillinger M, Merkel M, Schoenfuss M, Bohlen O, *et al*. Durability of lithium-ion 18650 cells under random vibration load concerning the inner cell design. J Energy Storage. 2020; 31: 101499. https://doi.org/10.1016/j.est.2020.101499

[24] Bangal OA, Chaturvedi V, Babu PKA, Shelke MV. Impedance analysis and equivalent circuit modelling of cells subjected to sinusoidal vibration test using electrochemical impedance spectroscopy. In: 2019 IEEE Transportation Electrification Conference (ITEC-India); 2019 Dec 17-19; Bengaluru, India. https://doi.org/10.1109/ITEC-India48457.2019.ITECINDIA2019-232

[25] Xu X, Tang S, Han X, Wu Y, Lu L, Liu X, *et al*. Anomalous calendar aging of Ni-rich cathode batteries: focusing on structural degradation. Energy Storage Mater. 2024; 66: 103198. https://doi.org/10.1016/j.ensm.2024.103198

[26] Dubarry M, Qin N, Brooker P. Calendar aging of commercial Li-ion cells of different chemistries—a review. Curr Opin Electrochem. 2018; 9: 106-13. https://doi.org/10.1016/j.coelec.2018.05.023

[27] Zhang LW, Liu L, Terekhov A, Warnberg D, Zhao P. Thermal runaway of Li-ion battery with different aging histories. Process Saf Environ Prot. 2024; 185: 910-7. https://doi.org/10.1016/j.psep.2024.03.077

[28] Grimsmann F, Brauchle F, Gerbert T, Gruhle A, Parisi J, Knipper M. Impact of different aging mechanisms on the thickness change and the quick-charge capability of lithium-ion cells. J Energy Storage. 2017; 14: 158-62. https://doi.org/10.1016/j.est.2017.10.010

[29] Lang M, Darma MSD, Mereacre L, Liebau V, Ehrenberg H. Post mortem analysis of ageing mechanisms in LiNi0.8Co0.15Al0.05O2–LiNi0.5Co0.2Mn0.3O2–LiMn2O4/graphite lithium ion batteries. J Power Sources. 2020; 453: 227915. https://doi.org/10.1016/j.jpowsour.2020.227915

[30] Sarasketa-Zabala E, Gandiaga I, Rodriguez-Martinez LM, Villarreal I. Calendar ageing analysis of a LiFePO4/graphite cell with dynamic model validations: towards realistic lifetime predictions. J Power Sources. 2014; 272: 45-57. https://doi.org/10.1016/j.jpowsour.2014.08.051

[31] Nemati AB, Mousavi-Khoshdel SM, Molaeimanesh GR, Ebrahimi-Nejad S. Effects of ambient temperature on the health characteristics of vehicular Li-ion batteries by electrochemical impedance spectroscopy. J Therm Anal Calorim. 2021; 146: 665-72. https://doi.org/10.1007/s10973-020-10052-y

[32] Feng X, Zheng S, Ren D, He X, Wang L, Cui H, *et al*. Investigating the thermal runaway mechanisms of lithium-ion batteries based on thermal analysis database. Appl Energy. 2019; 246: 53-64. https://doi.org/10.1016/j.apenergy.2019.04.009

[33] Feng X, Zheng S, Ren D, He X, Wang L, Liu X, *et al*. Key characteristics for thermal runaway of Li-ion batteries. Energy Procedia. 2019; 158: 4684-9. https://doi.org/10.1016/j.egypro.2019.01.736

[34] Feng X, Ren D, He X, Ouyang M. Mitigating thermal runaway of lithium-ion batteries. Joule. 2020; 4: 743-70. https://doi.org/10.1016/j.joule.2020.02.010

[35] Zhang G, Wei X, Chen S, Wei G, Zhu J, Wang X, *et al*. Research on the impact of high-temperature aging on the thermal safety of lithium-ion batteries. J Energy Chem. 2023; 87: 378-89. https://doi.org/10.1016/j.jechem.2023.08.040

[36] Cai QS, Ji Q, Chen XP, Wang T, Li L, Yuan Q, *et al*. Comprehensive study of high-temperature calendar aging on cylinder Li-ion batteries. Chem Eng Sci. 2024; 298: 120355. https://doi.org/10.1016/j.ces.2024.120355

[37] Chombo PV, Laoonual Y. Quantification of heat energy leading to failure of 18650 lithium-ion battery abused by external heating. J Loss Prev Process Ind. 2022; 79: 104855. https://doi.org/10.1016/j.jlp.2022.104855

[38] Ubaldi S, Conti M, Marra F, Russo P. Identification of key events and emissions during thermal abuse testing on NCA 18650 cells. Energies. 2023; 16(7): 3250. https://doi.org/10.3390/en16073250

[39] Jones CM, Sudarshan M, García RE, Tomar V. Direct measurement of internal temperatures of commercially-available 18650 lithium-ion batteries. Sci Rep. 2023; 13: 14421. https://doi.org/10.1038/s41598-023-41718-w

[40] Ren D, Hsu H, Li R, Feng X, Guo D, Han X, *et al*. A comparative investigation of aging effects on thermal runaway behavior of lithium-ion batteries. eTransportation. 2019; 2: 100034. https://doi.org/10.1016/j.etran.2019.100034

[41] Zhang L, Liu J, Fan P, Du L, Ma Y, Qu B, *et al*. Unraveling the effect of short-term high-temperature storage on the performance and thermal stability of LiNi0.5Co0.2Mn0.3O2/graphite battery. J Power Sources. 2020; 459: 227842. https://doi.org/10.1016/j.jpowsour.2020.227842

[42] Zhang G, Wei X, Chen S, Wei G, Zhu J, Wang X, *et al*. Research on the impact of high-temperature aging on the thermal safety of lithium-ion batteries. J Energy Chem. 2023; 87: 378-89. https://doi.org/10.1016/j.jechem.2023.08.040

[43] Chen YQ, Kang YQ, Zhao Y, Wang L, Liu JL, Li YX, *et al*. A review of lithium-ion battery safety concerns: the issues, strategies, and testing standards. J Energy Chem. 2021; 59: 83-99. https://doi.org/10.1016/j.jechem.2020.10.017

[44] Mishra D, Tummala R, Jain A. Investigation of propagation of thermal runaway during large-scale storage and transportation of Li-ion batteries. J Energy Storage. 2023; 72: 108315. https://doi.org/10.1016/j.est.2023.108315

[45] Zhao LY, Li W, Luo WY, Zheng MX, Chen MY. Numerical study of critical conditions for thermal runaway of lithium-ion battery pack during storage. J Energy Storage. 2024; 84: 110901. https://doi.org/10.1016/j.est.2024.110901

[46] Zhang QS, Niu JH, Zhao ZH, Wang Q. Research on the effect of thermal runaway gas components and explosion limits of lithium-ion batteries under different charge states. J Energy Storage. 2022; 45: 103759. https://doi.org/10.1016/j.est.2021.103759

[47] Nie BS, Dong YS, Chang L. The evolution of thermal runaway parameters of lithium-ion batteries under different abuse conditions: a review. J Energy Storage. 2024; 96: 112624. https://doi.org/10.1016/j.est.2024.112624

[48] Barai A, Uddin K, Chevalier J, Chouchelamane GH, McGordon A, Low J, *et al*. Transportation safety of lithium iron phosphate batteries—a feasibility study of storing at very low states of charge. Sci Rep. 2017; 7: 5438. https://doi.org/10.1038/s41598-017-05438-2

[49] International Safe Transit Association (ISTA). ISTA 3E: Standard test method for performance testing of transport packaging for truckload shipments. East Lansing (MI): ISTA; 2017.

[50] Guddanti KP, Bharati AK, Nekkalapu S, Mcwherter J, Morris SL. A comprehensive review: impacts of extreme temperatures due to climate change on power grid infrastructure and operation. IEEE Access. 2025; 13: 49375-415. https://doi.org/10.1109/ACCESS.2025.3548531